Materials Science & Engineering A 596 (2014) 9–14

Contents lists available at ScienceDirect

Materials Science & Engineering A

journal homepage: www.elsevier.com/locate/msea

Austenite deformation behavior and the effect of ausforming process on martensite starting temperature and ausformed martensite microstructure in medium-carbon Si–Al-rich alloy steel

M. Zhang, Y.H. Wang, C.L. Zheng, F.C. Zhang, T.S. Wang *

State Key Laboratory of Metastable Materials Science and Technology, Yanshan University, Qinhuangdao 066004, China

ARTICLE INFO

Article history:
Received 25 October 2013
Received in revised form
29 November 2013
Accepted 29 November 2013
Available online 7 December 2013

Keywords:
Steel
Thermomechanical processing
Martensitic transformations
Microstructure
Hardness

ABSTRACT

Deformation behavior of austenite/supercooled austenite in a medium-carbon Si–Al-rich alloy steel is investigated on a thermomechanical simulator and an optical microscope. Effects of ausforming temperature, strain rate and strain on martensite start temperature (M_S) and ausformed martensite microstructure are studied in detail. Results show that power-law-type work hardening is caused during supercooled austenite deformation at 300 °C; and the work hardening followed by steady-state flow is caused during the deformation at 600 and 900 °C. The ausforming can decrease M_S, refined lath martensitic microstructure and slightly enhanced hardness. With decreasing the ausforming temperature the M_S and martensite lath thickness decrease markedly. The strain and strain rate do not have strong effects on the M_S and lath thickness. In addition, the ausforming can decrease the tetragonality of martensite and facilitate the formation of dislocation substructured martensite.

1. Introduction

Nanostructured bainite, which is composed of nanolaths of bainite and interlath films of retained austenite, can be prepared in high-carbon (~1 wt%) silicon-rich (> 1.5 wt%) alloy steels by austempering at low homologous temperatures (slightly more than martensite start temperature, M_S), showing an attractive combination of strength and toughness [1–4]. The nanostructured bainite forms on account of the low austempering temperature and the inhibition of cementite precipitation. The low austempering temperature requires decreased M_S, which can be achieved by high contents of carbon and substitutional alloy elements Mn, Ni, Cr and Mo, etc. The cementite precipitation can be inhibited by alloying with Si or Si+Al. Considering the poor weldability of high carbon steels, Yang and Bhadeshia [5] have made an attempt to prepare the nanostructured bainite in low-carbon steels by adding substitutional solutes to suppress the M_S and ensure austempering can be performed at lower temperatures. However, thick bainite laths were formed due to the coalescence of fine bainite laths during the austempering. Moreover, the present authors have obtained thicker bainite laths instead of nanostructured bainite laths in 60Si2CrV steel (~0.6 wt% C) by low-temperature austempering [6]. Recently, Lonardelli et al. [7] have synthesized nanostructured medium carbon bainitic steel (0.48 wt% C) by mechanical alloying followed by spark plasma sintering and isothermal heat treatment. The sintering process limits the austenite grain growth and suppresses the M_S, thus allowing the isothermal bainitic transformation at low temperatures and obtaining nanostructured bainite. Furthermore, the present authors have reported that plastic deformation of supercooled austenite can depress the M_S of medium-carbon Si–Al-rich steel [8], thus creating the nanostructured bainite in this steel by isothermal transformation at low temperatures [9]. Additionally, ausforming in unrecrystallized austenite region can enhance the strength and improve the toughness in low alloy bainitic/martensitic steels [10]. In this work, the effects of process parameters of austenite compression deformation, including deformation temperature, strain rate and reduction, on austenite deformation behavior and M_S were systematically studied. The aim is to accumulate the meaningful data for optimizing the process of austenite deformation and austempering to prepare nanostructured bainite in medium-carbon Si–Al-rich steel. In addition, the effect of the austenite deformation process on microstructure and hardness of ausformed martensite has been investigated.

2. Experimental procedure

Medium-carbon Si–Al-rich alloy steel was smelted in vacuum induction furnace and cast into a ~170 mm diameter ingot. The chemical composition is 0.51C–1.83Mn–1.76Cr–0.51Ni–2.01W–1.26Si–1.51Al–0.012P–0.010S (wt%), which was designed for preparing nanostructured bainite by low-temperature austempering

* Corresponding author. Tel.: +86 335 8074631; fax: +86 335 8074545.
E-mail address: tswang@ysu.edu.cn (T.S. Wang).

0921-5093/$ - see front matter © 2013 Elsevier B.V. All rights reserved.
http://dx.doi.org/10.1016/j.msea.2013.11.097

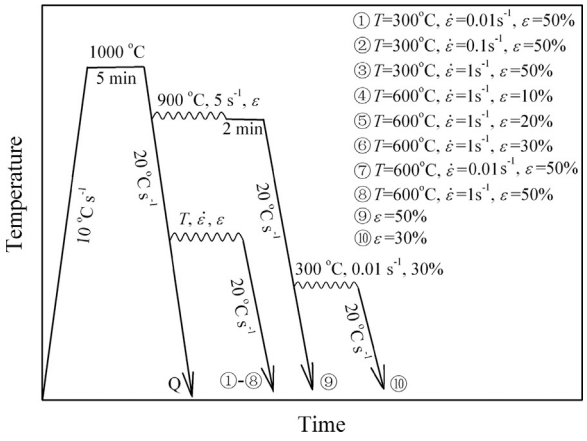

Fig. 1. Processing regimes.

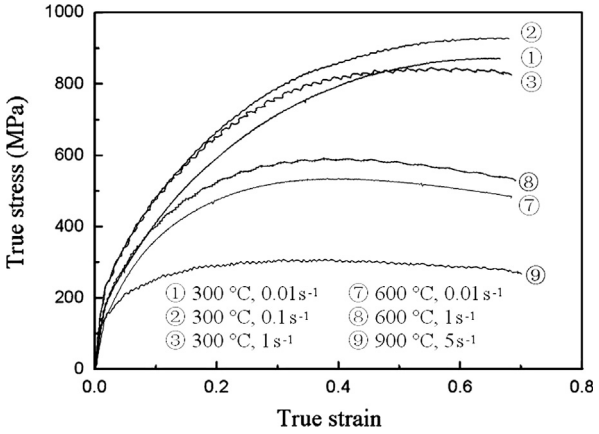

Fig. 2. Flow curves of austenite compressive deformation.

of deformed austenite. The ingot was homogenized and then forged into square bars with cross section dimension of 25 mm × 25 mm. Phase transformation temperatures, A_{c1} and A_{c3}, were measured as 745 and 830 °C, respectively, on a Netzsch DIL 402C/1/4/G thermal dilatometer. These bars were completely annealed at 920 °C for 1 h and furnace cooled to room temperature. Both uniaxially compressive deformation of austenite and martensitic transformation were performed on a Gleeble-3500 thermomechanical simulator using samples with dimensions of ⌀6 mm × 12 mm for the heating section and ⌀10 mm × 30 mm for the holding section. Process regimes used are defined in Fig. 1, which includes direct cooling of austenite (regime Q, unausformed process) and ausforming followed by cooling (regimes ①–⑩). After austenite deforming the load is not removed for regimes ① and ③–⑥, but removed for the other regimes. In the regimes ⑨ and ⑩, holding 2 min after compressive deformation at 900 °C is designed to refine austenite grains by static recrystallization. M_S temperatures were determined by dilation–temperature curves during cooling using the offset method. The dilation was measured along diameter by the C-Gauge. Microstructures were examined at the central area in the longitudinal section of thermomechanically processed samples by optical microscopy (OM, Axiover 200MAT), X-ray diffraction (XRD, Rigaku D/max-2500/PC), and transmission electron microscopy (TEM, JEM-2010), in order to avoid the disturbance caused by non-uniform deformation in the specimen. Samples used for OM and XRD were mechanically ground and polished, and then etched with 3% nital. Prior austenitic grain boundaries were displayed with an etchant composed of picric acid (1.4 g), sodium dodecyl benzene sulfonate (2 g), and distilled water (50 ml) by heating to ~70 °C in a waterbath for 2–3 min. XRD was operated in θ–2θ step scanning mode with a step width of 0.02° and a counting time of 2 s. Foils for TEM examination were sliced into ~0.5 mm thickness by wire electro-discharging and ground down to ~30 μm thickness by waterproof abrasive paper, and then thinned to perforation on a TenuPol-5 twinjet electropolishing device using an electrolyte composed of 7% perchloric acid and glacial acetic acid solution at room temperature and a voltage of ~32 V. The Vickers hardness was measured on a hardometer model of FM-ARS 9000 using a load of 1 kgf.

3. Results and discussion

3.1. Deformation behavior of austenite

Fig. 2 shows flow curves of austenite compressive deformation with regimes ①–③, ⑦–⑨. Regimes ①–③, ⑦ and ⑧ implement the deformation of supercooled austenite (300 and 600 °C). Regime ⑨ implements the deformation of stable austenite (900 °C). Power-law-type work hardening appears in the flow curves during deforming at 300 °C; and the work hardening followed by steady-state flow occurs during deforming at 600 and 900 °C. Thus, the austenite can be strengthened by the compressive deformation. The strengthening extent increases with decreasing deformation temperature. Serrations can be observed in every curve except curves ① and ⑦. The serrated flow curves reflect that the Portevin–LeChatelier (PLC) effect associated with dynamic strain ageing (DSA) occurs in the deformation of the supercooled austenite. From flow curves of supercooled austenite deformed at 300 and 600 °C, one can see that the critical strain for the onset of serration decreases with increasing strain rate, exhibiting an inverse PLC effect [11]. Under a strain rate 1 s^{-1} the critical strain for the onset of serration in curve ⑧ (deformed at 600 °C) is more than that in curve ③ (deformed at 300 °C), that is, the critical strain increases with increasing deformation temperature, also showing the characteristic of the inverse PLC effect [11].

Fig. 3a–f reveals typical OM micrographs of prior austenite grain boundaries in samples processed with regimes Q, ①, ③ and ⑦–⑨. Coarsely equiaxed prior austenite grains with mean size of 45 ± 15 μm form in the sample Q (Fig. 3a). Fine equiaxed prior austenite grains with mean size of 6 ± 3 μm form in the sample ⑨ (Fig. 3f) due to the static recrystallization of deformed austenite, which leads to the increase in austenite grain boundary area. Pancaked austenite grains form in samples ①, ③, ⑦ and ⑧ (Fig. 3b–e) due to the deformation at lower temperatures of 300 and 600 °C followed by rapid cooling, which will lead to the increase not only in dislocation density but also in boundary area.

3.2. Effect of austenite deformation regime on M_S

Dilation–temperature curves during cooling of austenite processed with various regimes are presented in Fig. 4. From these curves, M_S values of directly cooled austenite (regime Q) and deformed austenite (regimes ①–⑩) were determined and indicated in Table 1. For convenience, the processing parameters are also listed in the table. It is clear that M_S values of austenite deformed with regimes ①–⑩ (ranged in 200–268 °C) are much lower than that of directly cooled austenite (294 °C), suggesting that ausforming can suppress the M_S. The deformation temperature has a great effect on the M_S. The M_S decreases markedly with the decreasing deformation temperature. At a relatively low deformation temperature of 300 °C, the decrement of the M_S is reduced with increasing strain rate. However, approximately the same M_S values occur not only in regimes ② and ③ but also in regimes ⑦ and ⑧, respectively. Thus, the strain rate has little